AJNR Am J Neuroradiol 24:1869–1875, October 2003

Correlation of Early Dynamic CT Perfusion Imaging with Whole-Brain MR Diffusion and Perfusion Imaging in Acute Hemispheric Stroke

James D. Eastwood, Michael H. Lev, Max Wintermark, Clemens Fitzek, Daniel P. Barboriak, David M. Delong, Ting-Yim Lee, Tarek Azhari, Michael Herzau, Vani R. Chilukuri, and James M. Provenzale

BACKGROUND AND PURPOSE: **Compared with MR imaging, dynamic CT perfusion imaging covers only a fraction of the whole brain. An important assumption is that CT perfusion abnormalities correlate with total ischemic volume. The purpose of our study was to measure the degree of correlation between abnormalities seen on CT perfusion scans and the volumes of abnormality seen on MR diffusion and perfusion images in patients with acute large-vessel stroke.**

METHODS: **Fourteen patients with acute hemispheric stroke symptoms less than 12 hours in duration were studied with single-slice CT perfusion imaging and multislice MR diffusion and perfusion imaging. CT and MR perfusion studies were completed within 2.5 hours of one another (mean, 77 minutes) and were reviewed independently by two neuroradiologists. Hemodynamic parameters included cerebral blood flow (CBF), cerebral blood volume (CBV), and mean transit time (MTT). Extents of abnormality on images were compared by using Kendall correlation.**

RESULTS: **Statistically significant correlation was found between CT-CBF and MR-CBF abnormalities ($\tau = 0.60$, $P = .003$) and CT-MTT and MR-MTT abnormalities ($\tau = 0.65$, $P = .001$). Correlation of CT-CBV with MR-CBV approached significance ($\tau = 0.39$, $P = .06$). Extent of initial hyperintensity on diffusion-weighted images correlated best with extent of MR-CBV abnormality ($\tau = 0.69$, $P = .001$), extent of MR-MTT abnormality ($\tau = 0.67$, $P = .002$), and extent of CT-CBV abnormality ($\tau = 0.47$, $P = .02$).**

CONCLUSION: **Good correlation was seen between CT and MR for CBF and MTT abnormalities. It remains uncertain whether CT perfusion CBV abnormalities correspond well to whole-brain abnormalities.**

Several published studies have suggested that dynamic CT perfusion imaging with intravenous infusion of iodinated contrast material is a highly promising technique for the study of patients with acute stroke (1–8). However, dynamic CT perfusion studies presently are limited to either a 1-cm- or a 2-cm-thick section of tissue per acquisition, depending on whether a single-slice CT scanner or a multislice CT scanner is used. An underlying assumption regarding clinical use of CT perfusion imaging is that abnormalities seen in the small region of tissue studied with CT correlate with the full volume of ischemic tissue that can be seen with MR imaging. To date, we are not aware of any published data that correlate dynamic CT perfusion imaging abnormalities with full volumes of abnormality seen with MR diffusion and perfusion imaging. Such a study would, therefore, be valuable.

This study had two main aims. The first aim was to compare areas of cerebral blood flow (CBF), cerebral blood volume (CBV), and mean transit time (MTT) abnormalities seen on CT perfusion studies with the corresponding volumes of abnormality seen on MR perfusion studies. We hypothesized that significant

Received March 19, 2003; accepted after revision May 9.

Supported by GE Medical Systems (imaging), Bracco Diagnostics (contrast material), and Amersham Health (contrast material).

From the Departments of Radiology (J.D.E., D.P.B., J.M.P.), Community and Family Medicine (D.M.D.), and Medicine, Division of Neurology (V.R.C.), Duke University Medical Center, Durham, NC; the Division of Neuroradiology, Massachusetts General Hospital, Boston (M.H.L.); the Department of Diagnostic and Interventional Radiology, University Hospital, Lausanne, Switzerland (M.W.); the Department of Diagnostic and Interventional Radiology, Friedrich-Schiller University, Jena, Germany (C.F., T.A., M.H.); and Imaging Research Laboratories, John P. Robarts Research Institute, London, Ontario, Canada (T.Y.L.).

Address reprint requests to James D. Eastwood, MD, Box 3808, Duke University Medical Center, Durham, NC 27710-3808.

© American Society of Neuroradiology

correlation would be found between areas of abnormality detected on the CT perfusion studies and the volumes of abnormality found on the corresponding MR perfusion images. The second aim was to correlate extents of abnormality on CT perfusion scans with volume of abnormality present on MR diffusion images. We hypothesized that an area of CBF abnormality on CT perfusion scans would significantly correlate with volume of hyperintense abnormality on MR diffusion images.

Methods

Patients

Fifteen patients (seven women, eight men) with signs of acute hemispheric stroke were enrolled consecutively at five centers participating in a prospective trial to compare CT perfusion imaging with MR diffusion and perfusion imaging in patients with acute stroke. The mean age of the patients was 60.9 ± 19.6 years (range, 19–92 years). All patients had clinical findings suggestive of cortical ischemia at the time of diagnosis (ie, aphasia or hemineglect), as well as other typical findings of hemispheric stroke (eg, hemiparesis). For all patients, the clinical diagnosis of stroke was made by a neurologist with substantial experience with acute stroke. Symptom severity was measured by using the National Institutes of Health Stroke Scale (NIHSS) (11). The institutional review boards at all participating centers approved the protocol, and informed consent was obtained from the patients or their legal representatives before obtaining research images.

Imaging Protocol

All patients had symptom duration of less than 8 hours at the time research imaging was completed. Each patient first underwent clinical nonenhanced CT scanning of the brain to exclude hemorrhage. Consent for research scanning was then obtained from the patients or from their legal representatives. Next, patients underwent two research imaging examinations: a research CT examination consisting of CT angiography and CT perfusion imaging, and a research MR examination including MR angiography, diffusion-weighted imaging, and perfusion-weighted imaging. Availability of CT and MR units at the time informed consent was obtained was the main factor that determined which research examinations would be performed first. Thirteen patients underwent CT angiography and CT perfusion imaging before MR imaging and two patients underwent MR imaging before CT angiography and perfusion imaging. In all cases, the CT and MR research examinations were completed within 2.5 hours. One woman who initially received a diagnosis of acute stroke and who received intravenous recombinant tissue plasminogen activator (tPA) in the emergency department was discharged 2 days after admission with the diagnosis of somatiform disorder rather than stroke. In this case, the clinical nonenhanced CT scan was negative, and neither reader found any abnormalities on any of the research images obtained at the time therapy was begun. This patient was thus removed from the rest of the analysis. Thus, in total, 14 patients (six women, eight men) were included in the analysis of this study.

CT Angiography. Scanning consisted of helical acquisition with a commercially available scanner through the arteries of the circle of Willis during infusion of intravenous iodinated contrast material (100 or 150 mL) by using thin beam collimation (1–1.5 mm). CT angiography was performed to provide a control (along with MR angiography) for the possibility of early recanalization that could invalidate comparison of CT perfusion with MR diffusion and perfusion imaging.

CT Perfusion Imaging. Scanning consisted of continuous (cine) scanning (80 kVp, 200 mA) over one anatomic location (the level of the basal ganglia) of 5 or 10 mm thickness over 45 seconds during rapid infusion of 40 mL of intravenous contrast material of density 300 or 370 mg/dL. Data were reconstructed at 0.5 to 1.0 second intervals by using software available on the CT scanners. Infusion rate for contrast material during CT perfusion imaging ranged from 4 to 10 mL/s, and in all cases infusions were completed in less than 10 seconds.

MR Imaging. All patients underwent the following standard imaging sequences in the axial plane with a commercially available unit : nonenhanced T1-weighted, T2-weighted, and contrast material–enhanced T1-weighted sequences. All patients also underwent 3D time-of-flight MR angiography of the circle of Willis before gadolinium-based contrast material infusion.

Single-shot echo-planar diffusion-weighted imaging of the entire brain was performed by using three orthogonal acquisitions and averaging of these to produce trace-weighted diffusion-weighted images. The degree of diffusion weighting (b value) was 1000 s/mm^2. Mean TR was 8750 ms (range, 4000–12,000 ms), and mean TE was 99 ms (range, 98–100 ms).

Perfusion-weighted MR imaging was performed of approximately the superior one-half of the brain (eight sections) by using a T2*-weighted technique and rapid infusion (5 mL/s) of gadolinium-based contrast material (0.2 mmol/kg). Mean TR was 1433 ms (range 1200–1517 ms) and mean TE was 64 ms (range 29–90 ms), with 6.5-mm section thickness, and 1-mm section gap.

Image Analysis

Nonenhanced CT Scans. The initial clinical CT scans of the brain were evaluated by two experienced neuroradiologists working together at an imaging workstation and by using narrow window and level settings to optimize detection of acute stroke abnormalities (12). The presence of the following findings was noted and recorded: increased attenuation within an artery (eg, attenuated middle cerebral artery [MCA]), loss of insular ribbon, obscuration of basal ganglia, and regional (eg, wedge-shaped) low attenuation consistent with stroke.

CT Angiograms. All CT angiograms were reviewed by a single experienced neuroradiologist using an imaging workstation (Advantage Windows, GE Medical Systems, Milwaukee, WI) and software that displays three-dimensional data in multiple planes of section. The presence and locations of arterial occlusions and stenoses were recorded for each of the following: internal carotid artery (ICA), MCA, anterior cerebral artery (ACA), and posterior cerebral artery (PCA).

CT Perfusion Studies. All CT perfusion studies were independently reviewed by two experienced neuroradiologists using deconvolution-based commercial CT perfusion analysis software (CT Perfusion 2, GE Medical Systems). Maps of CBV, CBF, and MTT were created and studied visually by using a published method (2). Perfusion maps were displayed in three contrasting colors (red, yellow, and blue) with the abnormal values all displayed as a single color (eg, blue). The range of CBV values chosen to represent abnormally low values was 0–1.5 mL/100 g. The range of CBF values chosen was 0–10 mL/100 g/min. The range of MTT values chosen was all values greater than 6 seconds. Each reader independently determined whether an abnormality was present and measured the size of the apparent abnormality by drawing a region of interest (ROI) around the abnormality, determining the area contained within the ROI. Thus, for each case, areas of abnormality were determined for CBV, CBF, and MTT. For cases in which the readers disagreed about the presence of an abnormality, a consensus reading was subsequently performed.

MR Diffusion Studies. The diffusion-weighted images of all patients were examined by one neuroradiologist. For each section, ROIs were drawn by hand around regions having both hyperintensity and decreased apparent diffusion coefficient (ADC), based on visual inspection. The areas contained within

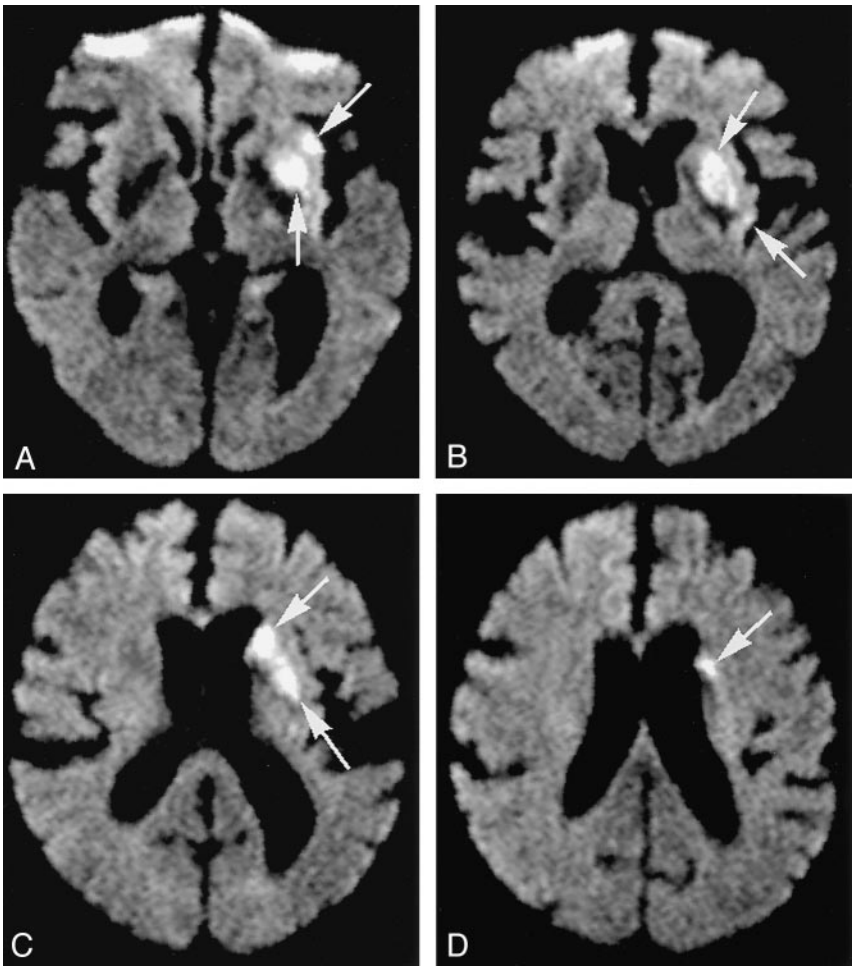

FIG 1. 54-year-old man with right hemiparesis.

A–D, Diffusion-weighted images (b = 1000 s/mm^2) illustrate volume of abnormality. Three-dimensional volume of abnormality was found by summing the areas of abnormality on each section (arrows) and multiplying by section thickness. The same approach was used to compute volumes of MR perfusion abnormality.

these ROIs were multiplied by the thickness of the section plus gap and added together to compute volume of abnormality (Fig 1). In our prior experience, we noted less than 5% intraobserver variability for this type of assessment. The area of the ROI and the mean value of ADC contained within it were recorded. The mean ADC value of the infarct for each patient was computed by taking the weighted average of the ADC value contained within ROIs on all sections.

MR Perfusion Studies. Each MR perfusion image was independently reviewed by the same two neuroradiologists who reviewed the CT perfusion scans. The method used to limit the influence of recall was to review the CT and MR perfusion images 60 days apart. Studies were analyzed by using commercially available deconvolution-based software (Functool PF; GE Medical Systems). Maps of relative CBV, relative CBF, and MTT were created. Because we have found that perfusion parameter values in white matter are less variable than those in gray matter, we used the white matter contralateral to the infarct as an internal reference. Values of relative CBV and relative CBF equal to or less than half those measured in the contralateral (normal) white matter above the lateral ventricles were considered to be abnormal. Values of MTT more than twice those found in the contralateral (normal) white matter were considered abnormal. The thresholds we used to define abnormality on the MR perfusion images were chosen because we have found that such values correspond well to the absolute values of perfusion parameters that we used for the CT perfusion scans. Color-coding was used for these thresholds in an identical manner as that used for the CT perfusion scans (eg, blue for low CBF). Each reader visually determined the area of abnormality on each section. The volume of abnormality was determined by multiplying the area of the abnormality on each section by the section thickness and gap and summing these values.

Statistical Methods

Kendall τ b correlation coefficients were computed to compare the extent of imaging abnormalities. To independently measure the correlation between CT perfusion and MR perfusion versus that of single-slice imaging and multislice imaging, the area of CBF abnormality on the single MR perfusion slice nearest to that of the CT perfusion slice was compared with both the single-slice CT-CBF abnormality and the full volume of MR perfusion abnormality. To measure the quality of fit of the regression between CT-CBF area and MR-CBF volume, the root mean deviation was computed. Pearson correlation coefficients were computed to compare the agreement between two readers. Statistical software used was SAS (SAS Institute, Cary, NC).

Results

The mean NIHSS score (± SD) was 12.6 ± 5.9. Two patients received intravenous tPA before research imaging and one patient received intraarterial tPA after research imaging. The decision to give tPA was made independent of the results of diffusion or perfusion imaging. The mean time from symptom onset to CT angiography and CT perfusion scanning was 3.1 hours. The mean time from symptom onset to MR imaging was 4.3 hours. The mean time separating

CT perfusion scanning from MR diffusion and perfusion scanning was 77 ± 31 minutes.

Nonenhanced CT Scans

In four patients, increased attenuation was seen in the ICA or MCA on the side of infarction. Four patients had either low attenuation in the basal ganglia or low attenuation in the insular cortex, or both, on the same side as infarction. Five patients had low-attenuation regions in cortical regions other than the insular cortex in the territory of one MCA. Three patients had no findings of acute stroke on the initial nonenhanced CT scan. Hemorrhage was not seen in any of the cases.

CT Angiography

Five patients had occlusion of the ICA on the side of infarction. Five patients had occlusion of the MCA on the side of infarction. Three patients had severe stenosis of the MCA on the side of infarction. One patient had moderate stenosis of the MCA on the side of infarction.

CT Perfusion Studies

Focal lesions were found on the CT-CBV maps in 10 of the 14 patients, including one of the three patients with normal nonenhanced CT scans. The mean size of CT perfusion CBV abnormalities was 10.0 ± 9.4 cm^2. The Pearson correlation coefficient comparing the two readers' visually measured regions abnormalities for CT-CBV maps was 0.53 ($P = .05$).

Focal lesions were found on the CT-CBF maps in 13 of the 14 patients, including two of the three patients with normal nonenhanced CT scans. The mean size of CT perfusion CBF abnormalities was 14.6 ± 12.3 cm^2. The Pearson correlation coefficient comparing the two readers' visually measured regions abnormalities for CT-CBF maps was 0.91 ($P = .0001$).

Focal lesions were found on the CT-MTT maps in all 14 patients. The mean size of CT perfusion MTT abnormalities was 27.1 ± 14.0 cm^2. The Pearson correlation coefficient comparing the two readers' visually measured CT-MTT abnormalities was 0.91 ($P = .0001$).

MR Angiography

Five patients had occlusion of the ICA on the side of infarction, five patients had occlusion of the MCA on the side of infarction, and four patients had severe stenosis of the MCA on the side of infarction. The results were essentially the same as those seen with CT angiography, with the sole exception being one patient who had moderate stenosis of one MCA seen on CT angiograms and severe stenosis of the same MCA seen on MR angiograms.

MR Perfusion Imaging

Focal lesions were found on the MR-CBV maps in 10 patients. The mean volume of MR perfusion CBV abnormalities was 38.7 ± 42.1 cm^3. The Pearson correlation coefficient comparing the extents of abnormality seen by the two readers for MR-CBV maps was 0.86 ($P = .0001$). Correlation of volume of MR-CBV abnormality with area of single-slice CT-CBV abnormality approached statistical significance ($\tau = 0.39$, $P = .06$).

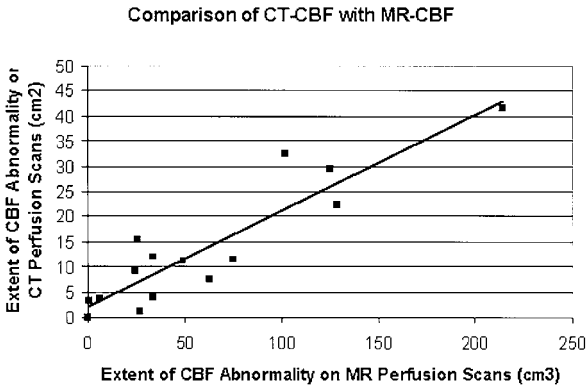

FIG 2. Scatterplot compares extents of CBF abnormality on single-slice CT perfusion scans with their corresponding extent of CBF abnormality on multislice MR perfusion images. Kendall τ b correlation coefficient for comparison of extent of CT-CBF with extent of MR-CBF was 0.60 ($P = .003$).

Focal lesions were found on the MR-CBF maps in 13 patients. The mean volume of MR perfusion CBF abnormalities was 64.8 ± 59.2 cm^3. Interreader agreement for MR-CBF maps as estimated by Pearson correlation was r = 0.55 ($P = .05$). Significant correlation was found between volume of MR-CBF abnormality and area of single-slice CT-CBF abnormality ($\tau = 0.60$, $P = .003$). Single-slice CT-CBF abnormality was significantly correlated with single-slice MR-CBF abnormality ($\tau = 0.52$, $P = .04$). Single-slice MR-CBF trended toward multislice MR-CBF abnormality ($\tau = 0.45$; $P = .08$). The root mean square deviation of the regression between CT-CBF and MR-CBF volume was 26.2 cm^2. Volume of MR-CBF abnormality is compared with area of single-section CT-CBF abnormality in Fig 2.

Focal lesions were found on the MR-MTT maps in all 14 patients. The mean volume of measured MR perfusion MTT abnormalities was 88.1 ± 80.1 cm^3. Interreader agreement for MR-MTT maps as estimated by Pearson correlation was 0.87 ($P = .0001$). Significant correlation was found between volume of MR-MTT abnormality and area of single-slice CT-MTT abnormality ($\tau = 0.65$, $P = .001$). Comparison of CT and MR perfusion imaging is illustrated in Fig 3.

MR Diffusion-Weighted Imaging

All 14 patients had regions of abnormality on initial diffusion-weighted images. The mean volume of abnormality was 50.7 ± 50.0 mL (range, 3.4–144.5 mL). The mean ADC value measured within regions of abnormality was 413 ± 151 × 10^{-6} mm^2/s (approximately 40% decrease). The CT perfusion parameter that correlated most highly with extent of MR diffu-

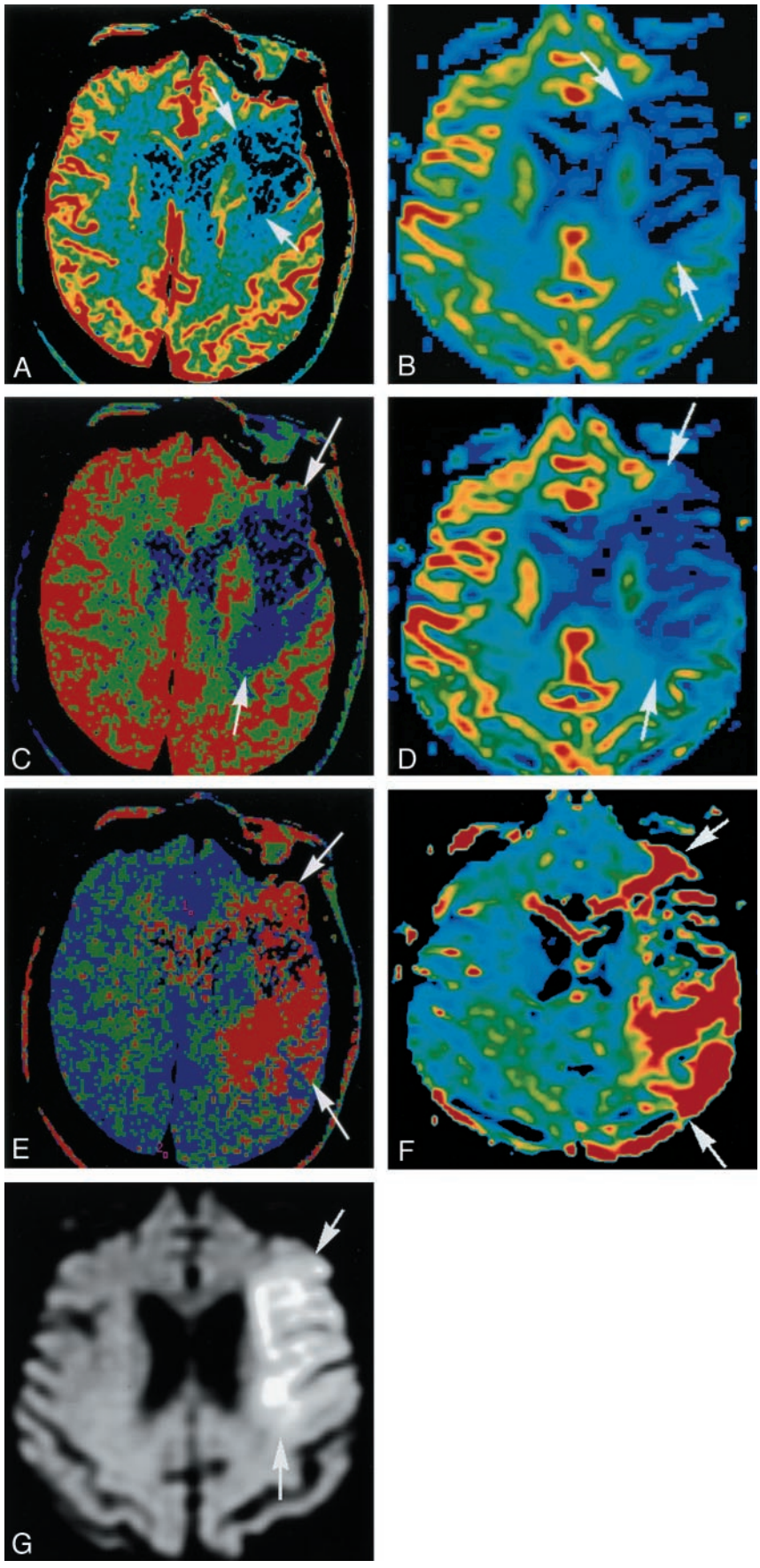

FIG 3. 90-year-old woman with acute right hemiparesis and aphasia 2 hours before imaging.

A, CT perfusion CBV map shows well-circumscribed area of very low CBV (arrows).

B, MR perfusion CBV map. Correlation of volume of MR-CBV abnormality with area of CT-CBV abnormality approached statistical significance in our study.

C, CT perfusion CBF map shows a larger abnormality than seen on the CBV map. CBF in the range of 0–10 mL/100 g/min is displayed as blue (arrows).

D, MR perfusion CBF map with areas of low relative CBF (< 50%) displayed as blue (arrows). Good correlation was found in our study between extents of 2D CT-CBF abnormality and 3D MR-CBF abnormality.

E, CT perfusion MTT map shows the largest extent of abnormality. Values of MTT greater than 6 seconds are displayed as red (arrows).

F, MR MTT map. Good correlation was found in our study between 2D CT-MTT abnormalities and 3D MR-MTT abnormalities (arrows).

G, Diffusion-weighted MR image (b = 1000 s/mm^2) obtained 4 hours after symptom onset through the basal ganglia shows abnormality in the left frontal lobe (arrows). Good correlation was found in our study between extent of CT-CBV abnormality and extent of diffusion-weighted abnormality. Good correlation was also found with extents of MR-CBV and MR-MTT abnormalities.

Statistical correlation of extents of CT and MR perfusion abnormalities with extent of initial abnormality on diffusion-weighted images

Perfusion Parameter	Correlation Coefficient*	*P* Value
CT-CBV	0.47	.02
CT-CBF	0.38	.05
CT-MTT	0.32	.11
MR-CBV	0.69	.001
MR-CBF	0.41	.04
MR-MTT	0.67	.002

* Kendall τ b correlation coefficients.

sion abnormality was area of decreased CT-CBV (τ = 0.47, P = .02). The MR perfusion parameter that correlated most highly with extent of MR diffusion abnormality was MR-CBV (τ = 0.74, P = .0003). The correlation statistics for each CT and MR perfusion parameter with diffusion abnormality are summarized in the Table.

Discussion

Dynamic CT perfusion imaging has shown substantial promise as a method for rapid assessment of cerebral hemodynamics in patients with stroke (1–8). However, the limitation in coverage inherent to the method (1–2 cm per acquisition) remains its most substantial technical limitation. Use of multislice CT scanners, which provide 2 cm of coverage per acquisition, and repeated acquisitions have been reported to result in coverage of up to 4 cm of brain tissue, still a small fraction of the total brain volume (3, 8). A major underlying assumption related to use of dynamic CT perfusion imaging in patients with stroke is that abnormalities seen on CT perfusion studies obtained from a small region of brain provide the physician with a fair estimate of the total volume of ischemic brain tissue present in a given patient. Our study sought to address this assumption by measuring the correlation between CT perfusion imaging abnormalities and volumes of abnormalities seen on MR diffusion and perfusion studies. We believed this measurement was essential since, if we found poor correlation (or no correlation), our result would dispel the argument for using CT perfusion as an alternative to MR imaging in patients with acute stroke. However, we believed that if we found strong correlation, our study might support more rapid development of a highly available tool for assessment of these patients.

Given this rationale, our study's finding of good correlation between abnormal areas on CT perfusion images and abnormal volumes on MR perfusion images for the parameters CBF and MTT is notable because it suggests that CT perfusion imaging provides an estimate of the full extent of ischemic tissue present. The lower degree of correlation seen between CT perfusion abnormalities and MR perfusion abnormalities for the CBV abnormalities suggests that the full volume of CBV abnormality may not be as reliably estimated by using single-slice CT perfusion imaging.

The good correlation between CBV abnormality (on both CT and MR images) and abnormality on diffusion-weighted images is notable because it supports the hypothesis that low CBV may be a marker for infarcted tissue that is similar to diffusion-weighted hyperintensity (8). This relationship may serve as the basis for an ischemic penumbra algorithm for CT (eg, CBF minus CBV, or MTT minus CBV).

Although we are not aware of previously published work that compares CT perfusion abnormalities with full volumes of MR-defined ischemic abnormalities, our study does substantially agree with previously published work. Wintermark et al compared CT perfusion imaging with MR diffusion imaging (3, 8) and MR perfusion imaging (8) within a 4-cm slab of brain tissue (the extent of brain coverage of the CT perfusion protocol used in those studies). The comparisons within those studies directly compared a small volume studied with CT perfusion imaging with the same small volume studied with MR diffusion and perfusion imaging (3, 8). The correlation between CT and MR in those previous studies was very high, as evidenced by very high Pearson correlation coefficients (0.95–0.97). Compared with the studies by Wintermark et al, our study measured lower coefficients of correlation between CT and MR. One reason may be our having available only single-slice CT scans to correlate with MR imaging. By comparison, Wintermark et al studied greater tissue with CT. One surprising finding was lower measured correlation between single-slice MR perfusion abnormality and volume of MR perfusion abnormality than single-slice CT perfusion abnormality and volume of MR perfusion abnormality. Differences in imaging angles and statistical variation are possible reasons for this discrepancy.

Although our study showed good correlation between early CT perfusion abnormalities and the full extent of ischemic tissue as seen on MR images, our study was limited in a number of ways that affect interpretation of results. First, our study was limited to a population of patients with proximal large-vessel (ICA and MCA) occlusion. It remains uncertain whether a study of a heterogeneous group of patients with small-vessel strokes or distal emboli would show similar correlation between CT and MR. Second, our study was a small one. Study of greater numbers of patients may help to clarify whether, for example, CBV changes can be as accurately estimated by using CT perfusion as CBF and MTT changes. Third, this study does not address the predictive value of dynamic CT perfusion imaging for final infarct size, infarct growth, and clinical outcome (eg, 90-day stroke severity score). These issues must be addressed before CT perfusion can be said to provide information similar to that provided by MR diffusion and perfusion imaging. We intend to study this issue in detail in our population. Finally, our study was completed at a time when many institutions did not routinely use multislice CT scanners to provide 2- or 4-cm coverage during CT perfusion scanning. Use of CT perfusion protocols with 2- or 4-cm coverage

would be expected to result in higher coefficients of correlation than those seen in our study (albeit by using higher doses of contrast material and radiation than those used in our study). We believe that strategies for increasing coverage of CT perfusion scans may be helpful, and physicians should seek to balance coverage, contrast material load, and radiation exposure when designing CT perfusion protocols for studying patients with stroke.

Conclusion

Our study provides new information relating early dynamic CT perfusion abnormalities with the full volume of abnormalities seen on early MR diffusion and perfusion images in patients with acute large-vessel stroke. Our data support further study of CT perfusion imaging for assessment of patients with acute stroke.

References

1. Lev MH, Segal AZ, Farkas J, et al. **Utility of perfusion-weighted CT imaging in acute middle cerebral artery stroke treated with intra-arterial thrombolysis: prediction of final infarct volume and clinical outcome.** *Stroke* 2001;32:2021–2028
2. Eastwood JD, Lev MH, Azhari T, et al. **CT perfusion scanning with deconvolution analysis: pilot study in patients with acute middle cerebral artery stroke.** *Radiology* 2002;222:227–236
3. Wintermark M, Reichhart M, Thiran J, et al. **Prognostic accuracy of cerebral blood flow measurement by perfusion computed tomography, at the time of emergency room admission, in acute stroke patients.** *Ann Neurol* 2002;51:417–432
4. Koenig M, Klotz E, Luka B, et al. **Perfusion CT of the brain: diagnostic approach for early detection of ischemic stroke.** *Radiology* 1998;209:85–93
5. Reichenbach JR, Rother J, Jonetz-Mentzel L, et al. **Acute stroke evaluated by time-to-peak mapping during initial and early follow-up perfusion CT studies.** *AJNR Am J Neuroradiol* 1999;20:1842–1850
6. Rother J, Jonetz-Mentzel L, Fiala A, et al. **Hemodynamic assessment of acute stroke using dynamic single-slice computed tomographic perfusion imaging.** *Arch Neurol* 2000;57:1161–1166
7. Mayer TE, Hamann GF, Baranczyk J, et al. **Dynamic CT perfusion imaging of acute stroke.** *AJNR Am J Neuroradiol* 2000;21:1441–1449
8. Wintermark M, Reichhart M, Cuisenaire O, et al. **Comparison of admission perfusion computed tomography and qualitative diffusion- and perfusion-weighted magnetic resonance imaging in acute stroke patients.** *Stroke* 2002;33:2025–2031
9. Wintermark M, Thiran JP, Maeder P, Schnyder P, Meuli R. **Simultaneous measurement of regional blood flow by perfusion CT and stable xenon CT: a validation study.** *AJNR Am J Neuroradiol* 2001;22:905–914
10. Furukawa M, Kashiwagi S, Matsunaga N, Suzuki M, Kishimoto K, Shirao S. **Evaluation of cerebral perfusion parameters measured by perfusion CT in chronic cerebral ischemia: comparison with xenon CT.** *J Comput Assist Tomogr* 2002;26:272–278
11. Brott T, Adams HP, Olinger CP, et al. **Measurements of acute cerebral infarction: a clinical examination scale.** *Stroke* 1989;20:864–870
12. Lev M, Farkas J, Gemmete J, et al. **Acute stroke: improved nonenhanced CT detection—benefits of soft-copy interpretation by using variable window width and center level settings.** *Radiology* 1999;213:150–155